

Dynamic Light Scattering Study of Temperature and pH Sensitive Colloidal Microgels

Valentina Nigro^{1a}, Roberta Angelini^{b,c}, Monica Bertoldo^d, Valter Castelvetro^e, Giancarlo Ruocco^{c,f}, Barbara Ruzicka^{b,c}

^a*Dipartimento di Fisica, Università degli Studi di Roma Tre, Via della Vasca Navale 84, 00146 Roma, Italy.*

^b*Istituto per i Processi Chimico-Fisici del Consiglio Nazionale delle Ricerche (IPCF-CNR), UOS Roma, Pz.le Aldo Moro 5, I-00185 Roma, Italy.*

^c*Dipartimento di Fisica, Sapienza Università di Roma, Pz.le Aldo Moro 5, I-00185, Italy.*

^d*Istituto per i Processi Chimico-Fisici del Consiglio Nazionale delle Ricerche (IPCF-CNR), Area della Ricerca, Via G.Moruzzi 1, I-56124 Pisa, Italy.*

^e*Dipartimento di Chimica e Chimica Industriale, Università di Pisa, via Risorgimento 35, I-56126 Pisa, Italy.*

^f*Center for Life Nano Science, IIT@Sapienza, Istituto Italiano di Tecnologia, Viale Regina Elena 291, 00161 Roma, Italy.*

Abstract

Microgel particles composed of Interpenetrated Polymer Networks (IPN) of poly(N-isopropylacrylamide) (PNIPAM) and poly(acrylic acid) (PAAc) dispersed in water have been investigated through dynamic light scattering. The study of the temperature, concentration and pH dependence of the relaxation time has highlighted the existence of a thermoreversible transition corresponding to the swollen-shrunk volume phase transition. The presence of PAAc introduces an additional pH-sensitivity with respect to the temperature-sensitivity due to PNIPAM and leads to interesting differences in the transition process at acid and neutral pH.

Keywords: Colloidal dispersions - Microgels - Relaxation Dynamics - Dynamic Light Scattering

¹Corresponding author: valentina.nigro@gmail.com

1. Introduction

Colloidal systems have long been the subject of intense research either for theoretical implications and for technological applications. They are very good model systems for understanding the general problem of dynamic arrest, due to their larger tunability with respect to atomic and molecular glasses [1–4]. Moreover, thanks to their dimensions, colloidal systems can be easily investigated through conventional techniques, such as dynamic light scattering (DLS) and optical microscopy. The control of their interparticle potential [5] by tuning external parameters such as packing fraction, waiting time and ionic strength, has given rise to exotic phase diagrams with different arrested states (such as gels [6–8] and glasses [9, 10]) and unusual glass-glass transitions [11–13]. At variance with hard colloids soft colloids are characterized by an interparticle potential with a finite repulsion at or beyond contact. Theoretical studies [14–16] have indicated the existence of an even more complex phase behavior not experimentally reproduced up to now. Among soft colloidal systems microgels, aqueous dispersions of nanometre- or micrometre-sized hydrogel particles, allow furthermore to modulate the interaction potential through temperature and/or pH, unlike in ordinary colloids. Recent experimental studies have shown the evidence of unusual transitions between different arrested states [17] and the possibility to make strong glasses [18]. Moreover microgels have been largely studied in the last years because of their versatility and high sensitivity to external stimuli such as pH, temperature, electric field, ionic strength, solvent, external stress or light and are therefore particularly attractive smart materials [19–23]. Furthermore they find many applications in a lot of different fields such as in agriculture, construction, cosmetic and pharmaceuticals industries, in artificial organs and tissue engineering [20, 22, 24–29].

One of the most studied responsive microgel is based on the poly(N-isopropylacrylamide) also known as PNIPAM, a thermo-sensitive polymer. PNIPAM microgels were investigated for the first time in 1986 by Robert Pelton and Philip Chibante [30], since then they have been widely studied both experimentally and theoretically and a clear picture of preparation, characterization and applications has been provided [19, 20, 22, 23, 31]. PNIPAM microgels responsiveness is strongly dependent on the thermo-sensitivity of PNIPAM that presents a Lower Critical Solution Temperature in water at about 305 K. At room temperature indeed, it is found in a swollen state, the polymer is hydrophilic and a great amount of water is retained; by

increasing temperature above 308-311 K the polymer becomes hydrophobic, water is completely expelled and a shrunken state is found giving rise to a volume phase transition (VPT). As a result, any microgel based on PNIPAM undergoes the characteristic VPT due to the temperature sensitivity of PNIPAM [32]. Phase diagram [33, 34, 17] and important details on the gel structure of PNIPAM microgels near the volume phase transition have been obtained [35, 36]. It has been recently shown that the microgel swelling/deswelling behavior can be strongly affected by concentration [37, 17], by solvents [38] and by synthesis procedure such as growing number of cross-linking points [39, 40], different reaction pH conditions [41] or by introducing additives into the PNIPAM network [42].

In this context PNIPAM microgels containing another specie as co-monomer or interpenetrated polymer result to be even more interesting systems since they retain the main properties of the constituent polymer. In particular, adding acrylic acid (AAc) to PNIPAM microgel provides a pH-sensitivity to the system that leads to a more complex phase behavior. In this way a thermo and pH-sensitive system is obtained. As in the case of pure PNIPAM microgel a volume phase transition with temperature is observed, although with a remarkable reduction in the swelling capability as the AAc concentration is increased [43, 44]. Indeed the volume phase transition of these microgels is strongly dependent on the effective charge density controlled by the content of AAc monomer [43, 44], on the pH of the suspension [45–48] and on the salt concentration [45, 49]. In this framework the synthesis procedure plays an important role. Indeed, AAc can be incorporated into PNIPAM either by random copolymerization (PNIPAM-co-AAc) [45, 46, 48–53] or by polymer interpenetration (IPN PNIPAM-PAAc) [43, 47, 54–57]. In the first case particles are composed of a single network of both monomers, with properties dependent on the monomer ratio [45]. Conversely, in the second case microgels are made of two interpenetrated homopolymeric networks of PNIPAM and PAAc, with the same independent response as the two components to external stimuli [55]. This important characteristic of interpenetrating polymer network (IPN) microgels makes the mutual interference between the temperature-responsive and pH-responsive polymers largely reduced making the temperature dependence of the VPT unchanged with respect to the case of pure PNIPAM microgel (close to physiological temperature) and the IPN microgel more suitable for applications in controlled drug release and sensors [24, 58]. However investigations on IPN PNIPAM-PAAc microgels are scarce and only a preliminary temperature-concentration phase diagram has

been reported up to now [43], leaving unexplored the dependence on pH, ionic strength and crosslink density. A few investigations through DLS, rheology and microscopic techniques have confirmed the existence of the VPT transition [47, 54–57]. Nevertheless the scenario is far from being completely clear. Furthermore other open issues are related to the possibility to vary the *softness* of PNIPAM-PAAc microgel particles that makes this system a suitable and unique model to provide insights into the glass formation in molecular systems [18].

In this work, through DLS experiments, we study the dynamics of aqueous dispersions of IPN microgels of PNIPAM and PAAc as a function of temperature, pH, concentration and momentum transfer Q across the VPT transition. The relaxation time τ shows a clear dependence on temperature and new features related to both concentration and pH. Furthermore the investigation at different lengthscales has highlighted a $\tau \propto Q^{-n}$ dependence with $n > 2$. These results open the way to further investigations at different length and time scales.

2. Material and Methods

2.1. Materials

Materials. Both N-isopropylacrylamide (NIPAM) from Sigma-Aldrich and N,N'-methylene-bis-acrylamide (BIS) from Eastman Kodak were purified by recrystallization from hexane and methanol, respectively, dried under reduced pressure (0.01 mmHg) at room temperature and stored at 253 K until used. Acrylic acid (AAc) from Sigma-Aldrich was purified by distillation (40 mmHg, 337 K) under nitrogen atmosphere in the presence of hydroquinone and stored at 253 K until used. Sodium dodecyl sulphate (SDS), purity 98 %, potassium persulfate (KPS), purity 98 %, ammonium persulfate, purity 98 %, N,N,N',N'-tetramethylethylenediamine (TEMED), purity 99 %, ethylenediaminetetraacetic acid (EDTA), NaHCO_3 , were all purchased from Sigma-Aldrich and used as received. Ultrapure water (resistivity: 18.2 $\text{M}\Omega/\text{cm}$ at 298 K) was obtained with Sarium[®] pro Ultrapure Water purification Systems, Sartorius Stedim from demineralized water. All other solvents were RP grade (Carlo Erba) and were used as received. Before use dialysis tubing cellulose membrane, cut-off 14000 Da, from Sigma-Aldrich, was washed in running distilled water for 3 h, treated at 343 K for 10 min into a solution containing a 3.0 % weight concentration of NaHCO_3 and 0.4 %

of EDTA, rinsed in distilled water at 343 K for 10 min and finally in fresh distilled water at room temperature for 2 h.

Synthesis of IPN microgels. The IPN microgels were synthesized by a sequential free radical polymerization method: in the first step PNIPAM micro-particles were synthesized by precipitation polymerization and in the second step acrylic acid was polymerized into the preformed PNIPAM network [43]. (4.0850 \pm 0.0001) g of NIPAM, (0.0695 \pm 0.0001) g of BIS and (0.5990 \pm 0.0001) g of SDS were solubilized in 300 mL of ultrapure water and transferred into a 500 mL five-necked jacketed reactor equipped with condenser and mechanical stirrer. The solution was deoxygenated by bubbling nitrogen inside for 30 min and then heated at (273.0 \pm 0.3) K. (0.1780 \pm 0.0001) g of KPS (dissolved in 5 mL of deoxygenated water) was added to initiate the polymerization and the reaction was allowed to proceed for 4 h. The resultant PNIPAM microgel was purified by dialysis against distilled water with frequent water change for 2 weeks. The final weight concentration and diameter of PNIPAM micro-particles were 1.02 % and 80 nm (at 298 K) as determined respectively by gravimetric and DLS measurements. (65.45 \pm 0.01) g of the recovered PNIPAM dispersion and (0.50 \pm 0.01) g of BIS were mixed and diluted with ultrapure water up to a volume of 320 mL. The mixture was transferred into a 500 mL five-necked jacketed reactor kept at (295 \pm 1) K by circulating water and deoxygenated by bubbling nitrogen inside for 1 h. 2.3 mL of AAc and (0.2016 \pm 0.0001) g of TEMED were added and the polymerization was started with (0.2078 \pm 0.0001) g of ammonium persulfate (dissolved in 5 mL of deoxygenated water). The reaction was allowed to proceed for 65 min and then stopped by exposing to air. The obtained IPN microgel was purified by dialysis against distilled water with frequent water change for 2 weeks, and then lyophilized to constant weight. The poly(acrylic acid) content determined by acid/base titration was 6.6 % weight concentration (PAAc/IPN).

Sample preparation. IPN samples were prepared by dispersing lyophilized IPN into ultrapure water at weight concentration 1.0 and 3.0 % by magnetic stirring for at least 3 h. Samples at different concentrations were obtained by dilution.

Characterization. The poly(acrylic acid) content in 10 g of IPN dispersion was determined by addition of 11 mL of 0.1 M NaOH followed by potentiometric back titration with 0.1 M hydrochloric acid. Concentration of

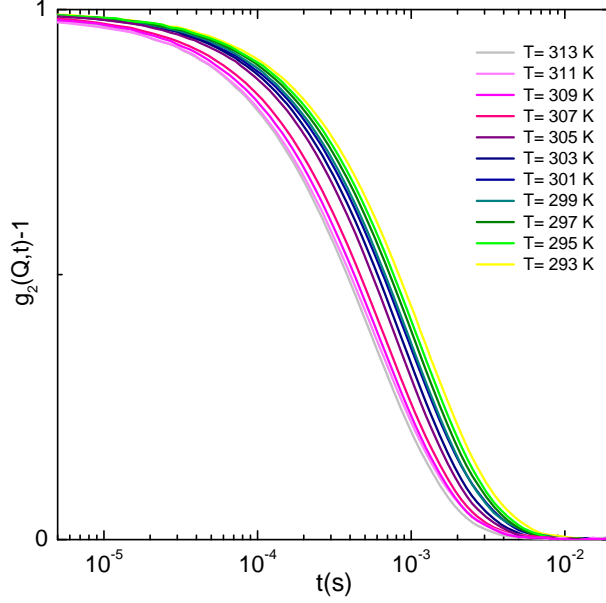


Figure 1: Normalized intensity autocorrelation functions collected at $\theta=90^\circ$ of an IPN sample at $C_w = 0.10$ % and pH 7 for the indicated temperatures.

dispersion was determined from the weight of the residuum after water removal by lyophilisation, corrected for the moisture residual amount obtained by thermogravimetric analysis (TGA). This was accomplished with a SII Nano-Technology EXTAR TG/DTA7220 thermal analyser at 275 K/min in nitrogen atmosphere (200 mL/min). 5 mg of sample in an alumina pan was analysed in the (313-473) K temperature range and the weight loss was assumed as moisture content.

2.2. Experimental Methods

In Fig. 1 the typical behavior of the normalized intensity autocorrelation functions for an IPN sample at weight concentration $C_w=0.10$ %, pH 7 and $\theta=90^\circ$ for the indicated temperatures is shown. DLS measurements have been performed with a multiangle light scattering setup. The monochromatic and polarized beam emitted from a solid state laser with a wavelength $\lambda=642$ nm and a power of 100 mW is focused on the sample placed in a cylindrical VAT for index matching and temperature control. The scattered intensity is collected at five different values of the scattering angle $\theta=30^\circ, 50^\circ, 70^\circ, 90^\circ, 110^\circ$, that correspond to five different values of the momentum transfer Q , accord-

ing to the relation $Q=(4\pi n/\lambda) \sin(\theta/2)$. Single mode optical fibers coupled to collimators collect the scattered light as a function of time and scattering vector. In this way one can measure simultaneously the normalized intensity autocorrelation function $g_2(Q, t) = \langle I(Q, t)I(Q, 0) \rangle / \langle I(Q, 0) \rangle^2$ at five different Q values with an high coherence factor close to the ideal unit value. Measurements have been performed as a function of temperature across the VPT. As commonly known the intensity correlation functions of most colloidal systems cannot be well described through a single exponential decay but the Kohlrausch-Williams-Watts expression [59, 60] is generally used:

$$g_2(Q, t) = 1 + b[e^{-(t/\tau)^\beta}]^2 \quad (1)$$

where b is the coherence factor, τ is an "effective" relaxation time and β generally describes the deviation from the simple exponential decay ($\beta = 1$). The different relaxation time present in glassy materials lead to a stretching of the correlation functions (here referred to as "stretched behavior") characterized by an exponent $\beta < 1$ which can be related to the distribution of the relaxation times. In the case of Brownian diffusion it is possible to relate the relaxation time to the translational diffusion coefficient D_t through the relation $\tau = 1/(Q^2 D_t)$. In the limit of non interacting spherical particles the Stokes Einstein relation $R = K_B T / 6\pi\eta D_t$ allows, known the viscosity η , to calculate the hydrodynamic radius from the diffusion coefficient.

In Fig. 2 the temperature dependence of R at pH 7 normalized with respect to the value $R = (188.3 \pm 0.6) \text{ nm}$ at $T = 297 \text{ K}$ is shown together with the results from previous works at different concentrations [47, 18]. In the inset of Fig. 2 the comparison between our results obtained for pH 7 and pH 5 (using $R = (135.2 \pm 0.5) \text{ nm}$ at $T = 297 \text{ K}$) is also shown. The hydrodynamic radii of this work have been calculated by using the viscosity of the solvent. Our results are in agreement with previous works [47, 18] with a slight discrepancy at high temperatures above the VPT. This can be attributed to different reasons: the approximation of using the solvent viscosity and the possible failure of the Stokes-Einstein relation in the shrunken high temperature state due to non spherical and/or interacting particles. For all these reasons in the following we will always refer to the behavior of the relaxation time rather than to the hydrodynamic radius.

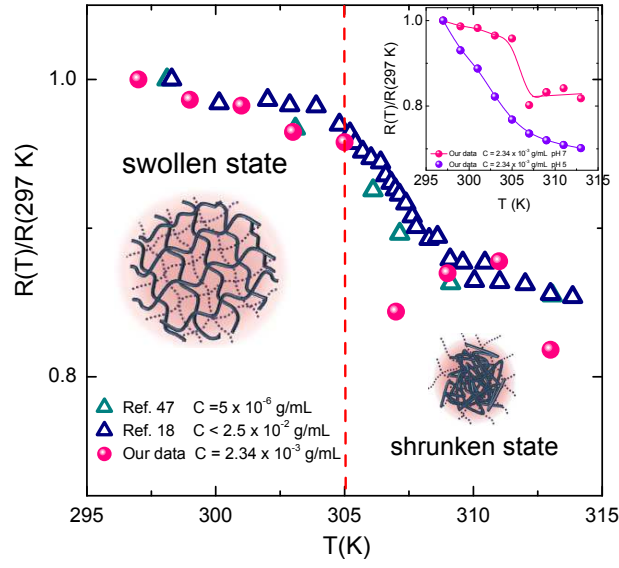


Figure 2: Normalized radius as obtained from DLS measurements for an IPN sample at $C_w = 0.10\%$ (equivalent to a weight/volume concentration of 2.34×10^{-3} g/mL), pH 7 and $\theta=90^\circ$ compared with results from ref. [47, 18]. Inset: comparison between our results for the temperature dependence of the normalized radius at pH 7 and at pH 5. Full lines are guides to the eyes.

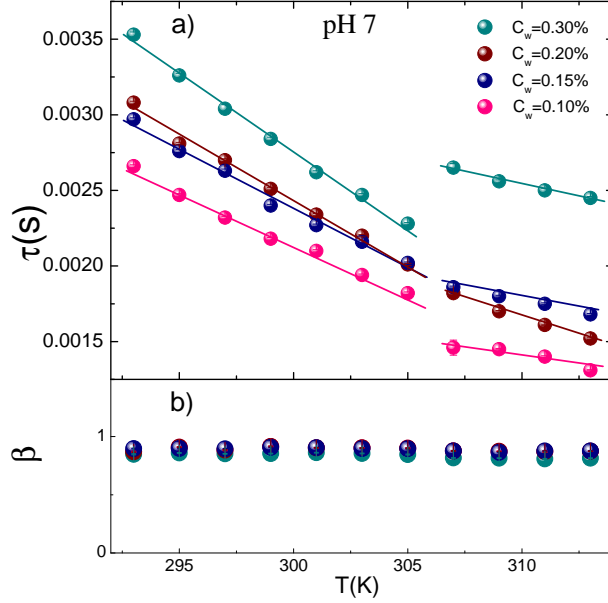


Figure 3: (a) Relaxation times and (b) stretching parameter from Eq. 1 as a function of temperature at pH 7 for the indicated concentrations. Full lines in (a) are guides to the eyes.

3. Results and Discussion

The DLS technique has been used to characterize the swelling behavior of the IPN microgel in the temperature range $293 \text{ K} \leq T \leq 313 \text{ K}$ where the volume phase transition is expected to occur. In order to neglect interparticle interactions and avoid phase separation diluted solutions at four different weight concentrations $C_w = 0.10\%$, $C_w = 0.15\%$, $C_w = 0.20\%$, $C_w = 0.30\%$ have been studied. To test reproducibility measurements have been repeated several times. The pH dependence of the suspensions has been investigated both for acid and neutral solution at pH 5 and 7, respectively. In this way a clear picture of the microgel behavior as a function of temperature, pH and concentration is drawn. In Fig. 1 the intensity correlation functions show a clear transition occurring above $T = 305 \text{ K}$. The volume phase transition from a swollen to a shrunken state is associated to a dynamical transition evidenced by looking at the relaxation time obtained through a fit of the intensity correlation functions according to Eq. 1. Its behavior with temperature is reported in Fig. 3: as temperature is increased the relaxation time shows a slight decrease until the transition is approached around 305 K.

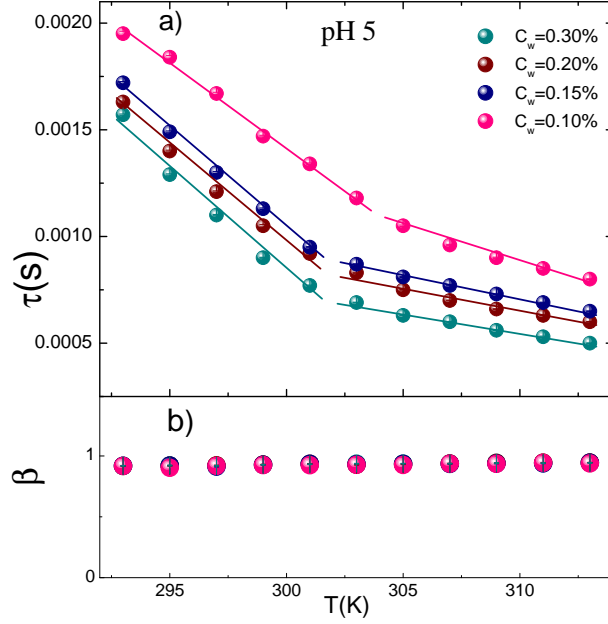


Figure 4: (a) Relaxation times and (b) stretching parameter from Eq. 1 as a function of temperature at pH 5 for the indicated concentrations. Full lines in (a) are guides to the eyes.

Thereafter, depending on concentrations, different behaviors are observed. For the lowest concentrated sample at $C_w=0.10\%$ after 305 K the relaxation time abruptly reaches its lowest value, corresponding to a transition of the microgel particles from the swollen to the shrunken state. The aforementioned transition of IPN has been reported to be smoother with respect to the case of pure PNIPAM microgel due to the presence of the acrylic acid that makes the swelling capability of the microgel greatly reduced [43, 47, 48]. Our results indicate that at increasing concentration the jump becomes smaller and smaller with an interesting swap in trend for the highest concentrated sample at $C_w=0.30\%$. Moreover, at increasing concentration the relaxation time increases. On the contrary the stretching parameter β does not show any change with temperature and concentration, remaining just below one, indicating correlation functions slightly stretched.

This behavior is strongly affected by the pH of the solution as shown in Fig. 4 where relaxation time and stretching parameters as a function of temperature under acid conditions, at pH 5, are reported. At variance with neutral pH solutions in this case a sharp transition is never observed and as

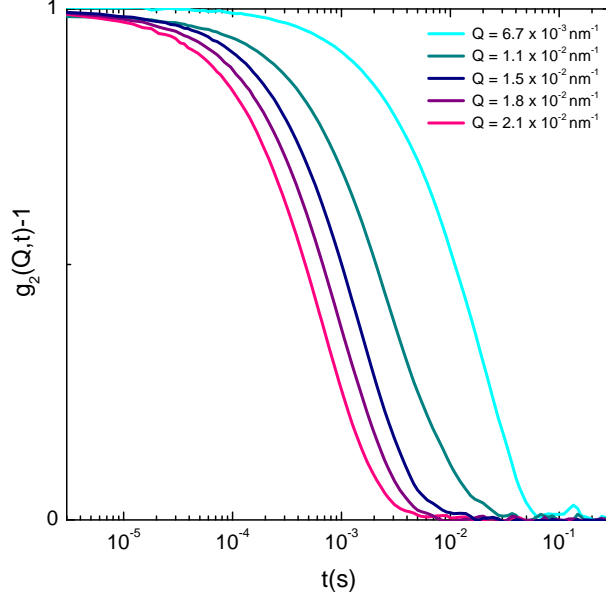


Figure 5: Normalized intensity autocorrelation curves at $C_w=0.20$ %, $T=303$ K and pH 7 for the indicated values of the exchanged momentum Q .

temperature is increased the relaxation time always decreases. Furthermore an opposite trend with respect to concentration is observed: with increasing concentration the relaxation time decreases. The comparison between Fig. 3a and Fig. 4a shows also that the relaxation times are always smaller in acid conditions. As in the case of neutral pH the stretching coefficient β is neither temperature nor concentration dependent and is always slightly below 1.

Therefore the pH of the solution strongly affects the relaxation times behavior: at neutral pH its values are higher and the transition appears to be more evident than in the case at acid pH. This dependence of the transition not only on concentration but also on pH confirms that the effect observed is due to the presence of PAAc. On the contrary the stretching parameter is insensitive even to pH changes.

To investigate the nature of the motion and to obtain information on different lengthscales we have studied the momentum transfer Q dependence of the relaxation time and stretching parameter. In Fig. 5 the normalized intensity correlation functions collected at different scattering angles for a sample at $C_w=0.20$ %, $T=303$ K and pH 7 are reported. The behaviors of relaxation time and stretching parameter as obtained through fits of the

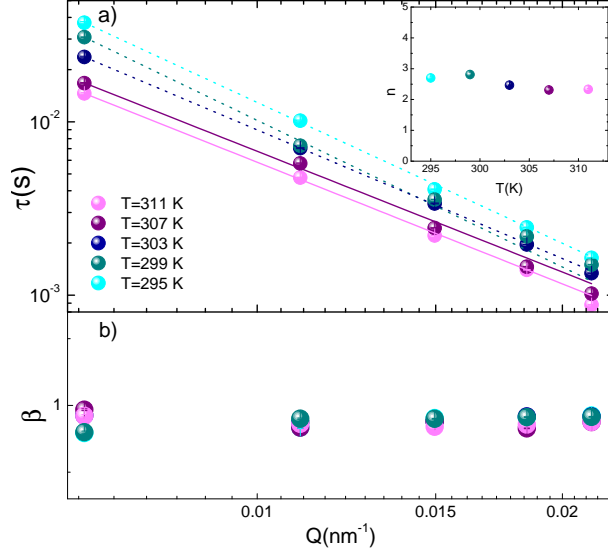


Figure 6: (a) Relaxation time and (b) stretching parameter from Eq. 1 as a function of momentum transfer Q at $C_w=0.10$ %, pH 7 for the indicated temperatures. Full lines are fits through Eq. 2 with $n=2.33 \pm 0.03$ ($T=311$ K), $n=2.31 \pm 0.07$ ($T=307$ K), $n=2.465 \pm 0.008$ ($T=303$ K), $n=2.81 \pm 0.08$ ($T=299$ K), $n=2.70 \pm 0.03$ ($T=295$ K). Inset: behavior of the exponent n as a function of temperature at $C_w=0.10$ % and pH 7.

autocorrelation curves according to Eq. 1 are shown as a function of the wave vector Q in Fig. 6.

The relaxation time, reported in a double logarithmic plot, is strongly Q dependent, with a typical power law decay described by the relation:

$$\tau = A Q^{-n} \quad (2)$$

where A is a constant and the exponent n defines the nature of the motion. In Fig. 6a the fits according to Eq. 2 (full lines) are superimposed to the data (symbols) and values of $n > 2$ (in particular n between 2 and 3) are found, in agreement with those reported in previous studies on the same microgel [18] and on different polymers [61, 62].

In Fig. 6b the stretching parameter β is reported, clearly showing no dependence on the wave vector Q .

4. Conclusions

The swelling behavior of the PNIPAM-PAAc IPN microgel has been studied as a function of temperature, pH, concentration and momentum transfer.

The presence of PNIPAM within the network determines the temperature sensitivity behavior and the addition of PAAc introduces an additional pH-sensitivity leading to interesting differences in the transition process at acid and neutral pH, respectively. In particular we have found that the dynamical transition evidenced by looking at the relaxation time is more pronounced at pH 7 with respect to pH 5 reflecting a discontinuous and a continuous volume phase transition respectively. Furthermore, while at neutral pH the relaxation time reaches the highest value at the highest concentration, at acid pH the dependence is inverted. Finally at neutral pH the relaxation time for the highest concentrated microgel shows, at odds with the low concentration samples, an intriguing increase after the VPT transition. This could be a precursor of the more complex behavior expected at even higher concentrations where a thermoreversible gelation should be observed [18]. It would be very interesting to address how the swelling capability and the gelation depend on PAAc concentration.

Acknowledgments

R.A. acknowledge support from MIUR-PRIN.

References

References

- [1] Sciortino F. and Tartaglia P. Glassy colloidal systems. *Adv. Phys.*, 54:471–524, (2005).
- [2] Trappe V. and Sandkühler P. Colloidal gels - low-density disordered solid-like states. *Curr. Opin. Colloid Interface Sci.*, 8:494, (2004).
- [3] Poon W.C.K. Phase separation, aggregation and gelation in colloid polymer mixtures and related systems. *Curr. Opin. Colloid Interface Sci.*, 3:593, (1998).
- [4] Zaccarelli E., Lu P. J., Ciulla F., Weitz D. A., and Sciortino F. *J. Phys.: Condens. Matter*, 20:494242, (2008).
- [5] Likos C. N. Effective interactions in soft condensed matter physics. *Physics Reports*, 348:267–439, (2001).
- [6] Lu P. J., Zaccarelli E., Ciulla F., Schofield A. B., Sciortino F., and Weitz D. A. *Nature*, 453:499–503, (2008).
- [7] Royall C.P., Williams S. R., Ohtsuka T., and Tanaka H. Direct observation of a local structural mechanism for dynamical arrest. *Nature Materials*, 7:556–561, (2008).
- [8] Ruzicka B., Zaccarelli E., Zulian L., Angelini R., Sztucki M., Moussaïd A., and Narayanan T. and Sciortino F. *Nat. Mater.*, 10:56, 2011.
- [9] Pusey P. N. and van Megen W. *Nature*, 320:340, 1986.
- [10] Imhof A. and Dhont J. K. G. Experimental phase diagram of a binary colloidal hard-sphere mixture with a large size ratio. *Physical Review Letters*, 75:1662–1665, 1995.
- [11] Pham K. N., Puertas A. M., Bergenholtz J., Egelhaaf S. U., Moussaïd A., Pusey P. N., Schofield A. B., Cates M. E., Fuchs M., and Poon W. C. K. Multiple glassy states in a simple model system. *Science*, 296:104, 2002.
- [12] Eckert T. and Bartsch E. Re-entrant glass transition in a colloid-polymer mixture with depletion attractions. *Phys. Rev. Lett.*, 89:125701, (2002).

- [13] Angelini R., Zaccarelli E., de Melo Marques F.A., Sztucki M., Fluerasu A., Ruocco G., and Ruzicka B. Glass-glass transition during aging of a colloidal clay. *Nat. Commun.*, (2014).
- [14] C. N. Likos, N. Hoffmann, H. Lowen, and A. A. Louis. Exotic fluids and crystals of soft polymeric colloids. *J. Phys. Cond. Matter*, 14:7681–7698, (2002).
- [15] P. E. Ramírez-González and M. Medina-Noyola. Glass transition in soft-sphere dispersions. *J. Phys. Cond. Matter*, 21:075101, (2009).
- [16] D. M. Heyes, S. M. Clarke, and A. C. Brank. Elasticity of compressed microgel suspensions. *J. Chem. Phys*, 131:204506, (2009).
- [17] Wang H., Wu X., Zhu Z., Liu C.S., and Zhang Z. Revisit to phase diagram of poly(n-isopropylacrylamide) microgel suspensions by mechanical spectroscopy. *J. Chem. Phys.*, 140:024908, (2014).
- [18] Mattsson J., Wyss H.M., Fernandez-Nieves A., Miyazaki K., Hu Z., Reichman D., and Weitz D.A. Soft colloids make strong glasses. *Nature*, 462(5):83–86, (2009).
- [19] Saunders B.R. and Vincent B. Microgels particles as model colloids: theory, properties and applications. *Adv. Colloid Interface Sci.*, 80:1–25, (1999).
- [20] Pelton R. Temperature-sensitive aqueous microgels. *Adv. Colloid Interface Sci.*, 85:1–33, (2000).
- [21] Vinogradov S.V. Colloidal microgels in drug delivery applications. *Curr. Pharm. Des.*, 12:4703–4712, (2006).
- [22] Das M., Zhang H., and Kumacheva E. Microgels: Old materials with new applications. *Annu. Rev. Mater. Res.*, 36:117–142, (2006).
- [23] Karg M. and Hellweg T. New “smart” poly(nipam) microgels and nanoparticle microgel hybrids: Properties and advances in characterisation. *Curr. Opin. Colloid Interface Sci.*, 14:438–450, (2009).
- [24] Park J.S., Yang H.N., Woo D.G., Jeon S.Y., and Park K.H. Poly(n-isopropylacrylamide-co-acrylic acid) nanogels for tracing and delivering

- genes to human mesenchymal stem cells. *Biomaterials*, 34:8819–8834, (2013).
- [25] Bajpai A.K., Shukla S.K., Bhanu S., and Kankane S. Responsive polymers in controlled drug delivery. *Prog. Polym. Sci.*, 33:1088–1118, (2008).
 - [26] Hamidi M., Azadi A., and Rafie. Hydrogel nanoparticles in drug delivery. *Adv. Drug Deliv. Rev.*, 60:1638–1649, (2008).
 - [27] Schexnailder P. and Schmidt G. Nanocomposite polymer hydrogels. *Colloid. Polym. Sci.*, 287:1–11, (2009).
 - [28] Smeets N.M.B. and Hoare T. Designing responsive microgels for drug delivery applications. *J. Polym. Sci. A Polym. Chem.*, 51:3027–3043, (2013).
 - [29] Su S., Monsur Ali Md., Filipe C.D.M., Li Y., and Pelton R. Microgel-based inks for paper-supported biosensing applications. *Biomacromolecules*, 9:935–9419, (2008).
 - [30] Pelton R.H. and Chibante P. Preparation of aqueous lattices with n-isopropylacrylamide. *Colloids Surf.*, 20:247–256, (1986).
 - [31] Lu Y. and Ballauff M. Thermosensitive core-shell microgels: From colloidal model systems to nanoreactors. *Prog. Polym. Sci.*, 36:767–792, (2011).
 - [32] Wu J., Huang G., and Hu Z. Interparticle potential and the phase behavior of temperature-sensitive microgel dispersions. *Macromolecules*, 36:440–448, (2003).
 - [33] Wu J., Zhou B., and Hu Z. Phase behavior of thermally responsive microgel colloids. *Phys. Rev. Lett.*, 90(4):048304, (2003).
 - [34] Paloli D., Mohanty P.S., Crassous J.J., Zaccarelli E., and Schurtenberger P. Fluid–solid transitions in soft-repulsive colloids. *Soft Matter*, (2012).
 - [35] Gao J. and Hu Z. Optical properties of n-isopropylacrilamide microgel spheres in water. *Langmuir*, 18:1360–1367, (2002).

- [36] Tang S. and Hu Z. Crystallization kinetics of thermosensitive colloids probed by transmission spectroscopy. *Langmuir*, 20:8858–8864, (2004).
- [37] Tan B.H., Pelton R.H., and Tam K.C. Microstructure and rheological properties of thermo-responsive poly(n-isopropylacrilamide) microgels. *Polymers*, 51:3238–3243, (2010).
- [38] Zhu P.W. and Napper D.H. Light scattering studies of poly(n-isopropylacrylamide) microgel particle in mixed water-acetic acid solvents. *Macromol. Chem. Phys.*, 200:1950–1955, (1999).
- [39] Kratz K. and Eimer W. Swelling properties of colloidal poly(n-isopropylacrylamide) microgels in solution. *Ber. Bunsenges. Phys. Chem.*, 102:848–854, (1998).
- [40] Kratz K., Hellweg T., and Eimer W. Structural changes in pnipam microgel particles as seen by sans, dls and em techniques. *Polymer*, 42:6631–6639, (2001).
- [41] Bao L. and Zhaj L. Preparation of poly(n-isopropylacrylamide) microgels using different initiators under various ph values. *Macromol. Sci.*, 43:1765–1771, (2006).
- [42] Hellweg T., Dewhurst C.D., Eimer W., and Kratz K. Pnipam-copolystyrene core-shell microgels: structure, swelling behavior, and crystallization. *Langmuir*, 20:4333–4335, (2004).
- [43] Hu Z. and Xia X. Hydrogel nanoparticle dispersions with inverse thermoreversible gelation. *Adv. Mater.*, 16(4):305–309, (2004).
- [44] Ma J., Fan B., Liang B., and XuJ. Synthesis and characterization of poly(n-isopropylacrylamide)/poly(acrylic acid) semi-ipn nanocomposite microgels. *J. Colloid Interface Sci.*, 341:88–93, (2010).
- [45] Kratz K., Hellweg T., and Eimer W. Influence of charge density on the swelling of colloidal poly(n-isopropylacrylamide-co-acrylic acid) microgels. *Colloids Surf. A*, 170:137–149, (2000).
- [46] Kratz K., Hellweg T., and Eimer W. Effect of connectivity and charge density on the swelling and local structure and dynamic properties of colloidal pnipam microgels. *Ber. Bunsenges. Phys. Chem.*, 102(11):1603–1608, (1998).

- [47] Xia X. and Hu Z. Synthesis and light scattering study of microgels with interpenetrating polymer networks. *Langmuir*, 20:2094–2098, (2004).
- [48] Jones C.D. and Lyon L.A. Synthesis and characterization of multiresponsive core-shell microgels. *Macromolecules*, 33:8301–8303, (2000).
- [49] Xiong W., Gao X., Zao Y., Xu H., and Yang X. The dual temperature/ph-sensitive multiphase behavior of poly(nisopropylacrylamide-co-acrylic acid) microgels for potential application in *in situ* gelling system. *Colloids Surf. B: Biointerfaces*, 84:103–110, (2011).
- [50] Meng Z., Cho J.K., Debord S., Breedveld V., and Lyon L.A. Crystallization behavior of soft, attractive microgels. *J. Phys. Chem. B*, 111:6992–6997, (2007).
- [51] Lyon L.A., Debord J.D., Debord S.B., Jones C.D., McGrath J.G., and Serpe M.J. Microgel colloidal crystals. *J. Phys. Chem. B*, 108:19099–19108, (2004).
- [52] Holmqvist P., Mohanty P.S., Nägele G., Schurtenberger P., and Heinen M. Structure and dynamics of loosely cross-linked ionic microgel dispersions in the fluid regime. *Phys. Rev. Lett.*, 109:048302, (2012).
- [53] Debord S.B. and Lyon L.A. Influence of particle volume fraction on packing in responsive hydrogel colloidal crystals. *J. Phys. Chem. B*, 107:2927–2932, (2003).
- [54] Xia X., Hua Z., and Marquez M. Physically bonded nanoparticle networks: a novel drug delivery system. *J. Control. Release*, 103:21–30, (2005).
- [55] Zhou J., Wang G., Zou L., Tang L., Marquez M., and Hu Z. Viscoelastic behavior and in vivo release study of microgel dispersions with inverse thermoreversible gelation. *Biomacromolecules*, 9:142–148, (2008).
- [56] Xing Z., Wang C., Yan J., Zhang L., Li L., and Zha L. pH/temperature dual stimuli-responsive microcapsules with interpenetrating polymer network structure. *Colloid Polym. Sci.*, 288:1723–1729, (2010).

- [57] Liu X., Guo H., and Zha L. Study of pH/temperature dual stimuli-responsive nanogels with interpenetrating polymer network structure. *Polymers*, 61(7):1144–1150, (2012).
- [58] Chen J.J. and Ahmad A.L. Ooi B.S. Poly(n-isopropylacrylamide-co-acrylic acid) hydrogels for copper ion adsorption: Equilibrium isotherms, kinetic and thermodynamic studies. *J. Env. Chem. Eng.*, 1:339–348, (2013).
- [59] Kohlrausch R. Thermoresponsive poly-(n-isopropylmethacrylamide) microgels: Tailoring particle size by interfacial tension control. *Pogg. Ann. Phys. Chem.*, 91:179–214, (1854).
- [60] Williams G. and Watts D.C. Non-symmetrical dielectric relaxation behavior arising from a simple empirical decay function. *J. Chem. Soc. Faraday Trans.*, 66:80–85, (1970).
- [61] Colmenero J., Alegría A., Alberdi J.M., Alvarez F., and Frick B. Dynamics of the α relaxation of a glass-forming polymeric system: Dielectric, mechanical, nuclear-magnetic-resonance, and neutron scattering studies. *Phys. Rev. B*, 44:7321–7329, (1991).
- [62] Colmenero J., Alegría A., and Arbe A. Correlation between non-debye behavior and q -behavior of the α -relaxation in glass-forming polymeric systems. *Phys. Rev. Lett.*, 69:478–481, (1992).